Available at www.sciencedirect.com

ScienceDirect

journal homepage: www.elsevier.com/locate/watres

Efficient recovery of nano-sized iron oxide particles from synthetic acid-mine drainage (AMD) water using fuel cell technologies

Shaoan Cheng [a,b], Je-Hun Jang [b,1], Brian A. Dempsey [b], Bruce E. Logan [b,*]

[a] State Key Laboratory of Clean Energy Utilization, Department of Energy Engineering, Zhejiang University, Hangzhou 310027, PR China
[b] Department of Civil and Environmental Engineering, 212 Sackett Building, Penn State University, University Park, PA 16802, United States

ARTICLE INFO

Article history:
Received 11 April 2010
Received in revised form
15 July 2010
Accepted 19 July 2010
Available online 27 July 2010

Keywords:
AMD
Energy
Iron oxide
Microbial fuel cell
Particles

ABSTRACT

Acid mine drainage (AMD) is an important contributor to surface water pollution due to the release of acid and metals. Fe(II) in AMD reacts with dissolved oxygen to produce iron oxide precipitates, resulting in further acidification, discoloration of stream beds, and sludge deposits in receiving waters. It has recently been shown that new fuel cell technologies, based on microbial fuel cells, can be used to treat AMD and generate electricity. Here we show that this approach can also be used as a technique to generate spherical nanoparticles of iron oxide that, upon drying, are transformed to goethite (α-FeOOH). This approach therefore provides a relatively straightforward way to generate a product that has commercial value. Particle diameters ranged from 120 to 700 nm, with sizes that could be controlled by varying the conditions in the fuel cell, especially current density (0.04–0.12 mA/cm^2), pH (4–7.5), and initial Fe(II) concentration (50–1000 mg/L). The most efficient production of goethite and power occurred with $pH = 6.3$ and Fe(II) concentrations above 200 mg/L. These results show that fuel cell technologies can not only be used for simultaneous AMD treatment and power generation, but that they can generate useful products such as iron oxide particles having sizes appropriate for used as pigments and other applications.

1. Introduction

Acid-mine drainage (AMD) and acid rock drainage (ARD) are caused by the oxidation of pyrite and other sulfidic minerals when they are exposed to air and water due to mining or excavation operations. Both types of discharges will be referred to as AMD in this paper. AMD waters contain high concentrations of mineral acid, dissolved Fe(II), and sulfates, as well as a variety of toxic chemicals such as lead, copper, cadmium, and arsenic. AMD can be difficult and costly to treat. Treatment is usually accomplished with passive systems for low-flow abandoned discharges, and active processes for regulated discharges. Most active treatment involves a rapid increase in pH (lime, caustic, or other base) followed by agitation and energy-intensive forced aeration. In a few instances the iron oxides have been recovered for use as pigments, magnetic materials and catalysts (Kirby et al., 1999; Kairies et al., 2005; Wei and Viadero, 2007) or for fluoride or arsenate removal (Zhao and Stanforth, 2001; Luengo et al., 2007). However, the resulting sludge can be highly variable

---

[*] *Corresponding author*. Tel.: +1 814 863 7908.
E-mail address: blogan@psu.edu (B.E. Logan).
[1] Present address: Sandia National Laboratories, Carlsbad Programs Group, 4100 National Parks Highway, Carlsbad, NM 88220, United States

0043-1354/$ – see front matter © 2010 Elsevier Ltd. All rights reserved.
doi:10.1016/j.watres.2010.07.054

in composition and can contain magnesium, aluminum, other metals, and organic materials, making resource recovery problematic (Kirby et al., 1999; Matlock et al., 2002). Additional processes such as selective precipitation (Matlock et al., 2002; Wei et al., 2005; Jenke and Diebold, 1983; Tabak et al., 2003) may be required to produce marketable products.

An alternative approach for treating AMD was recently proposed based on the use of a new type of fuel cell architecture called an AMD fuel cell (AMD-FC) (Cheng et al., 2007). This device is based on a microbial fuel cell (MFC) that is being developed for power generation from the microbial oxidation of dissolved organic or inorganic matter. The use of an AMD-FC has the advantages of generating electricity, while at the same time treating the AMD (Cheng et al., 2007). During treatment, ferrous iron is oxidized in the anode chamber under anoxic conditions, while at the cathode oxygen is reduced to water. Our previous studies showed that ferrous iron was completely removed through oxidation to insoluble Fe(III), and that it formed a precipitate on the bottom of the anode chamber (Cheng et al., 2007). This suggested to us that such a process might be useful for obtaining more controlled conditions for iron oxide production. We therefore examined the composition of the iron oxide formed in this process, and we show here that particle size can be controlled by varying the current density (through variation in the load), pH, and iron concentration.

2. Methods

AMD-FCs were constructed as previously described (Cheng et al., 2007), with two chambers each 14 mL in volume separated by an anion exchange membrane. Both electrodes were made from carbon cloth with a projected surface area of 7 cm^2, and the cathode contained a Pt catalyst (0.5 mg/cm^2). The anode and cathode chambers were filled with deionized water containing NaCl (0.05 M, to increase solution conductivity) and $NaHCO_3$ (0.06 M, pH buffer), and then sparged with CO_2 for 0.5 h to adjust the pH and remove dissolved oxygen. $FeSO_4$ was added to the anode chamber at 400 mg/L in an anaerobic glove box and the pH adjusted to 6.3 (except as noted) using HCl (0.1 M) under conditions of continuous CO_2 sparging. The AMD-FCs (duplicate reactors) were then placed in a temperature controlled room (30 °C), and left in open circuit mode for 0.5 h before connecting the circuit containing a resistor (1000 Ω in all experiments except as noted). The medium in the reactor was refilled when the cell voltage dropped below ˜1 mV, which varied depending on conditions from 5 to 25 h. Particles on the anode surface were removed with a plastic plate and added to the anode solution, and then this solution was analyzed for particle sizes. To determine the effect of operating conditions on iron oxide production, the external resistance was varied from 100 to 2000 Ω, pH from 4 to 7.5, and ferrous iron from 0.9 to 17.9 mM. After each cycle of current generation, the solution was replaced with fresh media.

The anode solutions were sonicated to disperse the particles (5 min, 1510R-MTH, Branson Sonicator, USA) and then analyzed for their particle size distribution (Zeta Sizer, Malvern Instruments Limited, UK). The particles were washed (deionized water) and centrifuged (2400*g*) three times and dried in air at 40 °C. Mössbauer spectra were obtained at room temperature using constant acceleration and a $^{57}Co/Rh$ source of 25 mCi initial activity (Jang et al., 2003). The computer program "*Recoil*" (Lagarec and Rancourt, 1998) was used to analyze the velocity distributions. XRD was performed with an X'PERT Phillips four circle diffractometer using CuKa radiation. The powder sample was re-dispersed in ethanol, sonicated, and settled onto a highly oriented pyrolytic graphite disc for AFM observation (BioScopeAFM, Digital Instrument, Santa Barbara, CA, Nanoscope IIIa control system version 4.32r3).

3. Results and discussion

Under the baseline conditions of pH = 6.3 and 7 mM of ferrous iron, the AMD-FC produced a current density of 640 mA/m^2 (290 mW/m^2) as previously reported (Cheng et al., 2007). During the period of electricity production, a red precipitate was observed in the anode solution and on the anode surface, and the columbic efficiency was almost 100% as previously reported (Cheng et al., 2007), indicating that all the particles were likely precipitated through the same mechanism. The Mössbauer spectrum showed a paramagnetic doublet at room temperature, with parameters indicating presence of ferrihydrite or nano-sized goethite (Fig. 1) (Govaert et al., 1976). XRD patterns indicated the precipitate contained nano-sized goethite (α-FeOOH) (Penn et al., 2006), which is indiscernible from ferrihydrite on room-temperature Mössbauer spectroscopy because of the lack of magnetic ordering (Fig. 2) (Burleson and Penn, 2006). No other forms of ferric oxides were observed in the precipitate. AFM images showed the goethite particles were highly spherical, with a particle size of 402 ± 20 nm under these conditions (Fig. 3). Goethite particles are usually synthesized through titration using either ferric or ferrous salt solutions. This approach produces particles with a needle-shaped morphology (Kosmulski et al., 2004). In some cases, such as in the presence of polymer templates, some goethite particles can be formed that have a spherical shape (Sepulveda-Guzman et al., 2005). In our case, all synthesized particles showed highly spherical shapes across the complete size range obtained here under the studied conditions. This

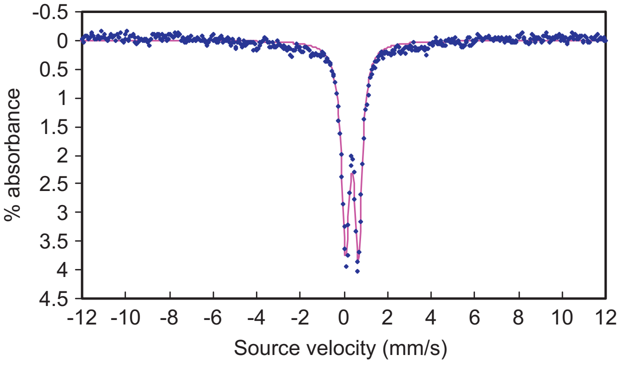

Fig. 1 – Mössbauer spectrum of the sample measured at room temperature (295 K), sample prepared at 0.05 M NaCl, 0.06 M $NaHCO_3$, 0.007 M Fe^{2+}, pH = 6.3, and 1 kΩ external resistance.

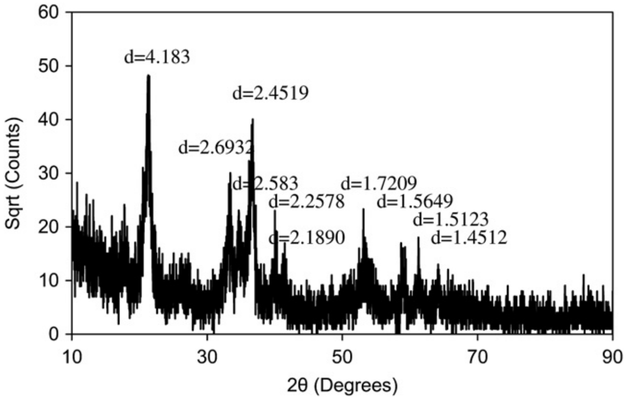

Fig. 2 – XRD pattern of the prepared sample under conditions of 0.05 M NaCl, 0.06 M $NaHCO_3$, 0.007 M Fe^{2+}, pH = 6.3, and 1 kΩ external resistance.

relatively uniform shape was likely a result of the electrochemical precipitation process used here, compared to more commonly used titration processes. Further investigation of the mechanism of particle formation is needed.

Particle sizes could be varied from 120 to 700 nm by changing the operating conditions of the AMD-FCs. Increasing the current from 0.04 to 0.12 mA/cm^2 (by varying the external resistance from 2000 to 200 Ω) decreased the average particle sizes formed in the reactor from 700 ± 50 to 450 ± 60 nm (Fig. 4A), as a result of the increased current which produced a faster rate of nucleation (Kim et al., 2004). The particle size distribution also became narrower with increased current. These two results indicate that current both increased particle size was due to both the increased rate of ferrihydrite nucleation as well as coalescence of smaller particles.

The smallest particles of 120 nm were formed at a pH = 4, likely as a result of the slow oxidation rate and low cell voltage under these conditions (Cheng et al., 2007). The particle size distribution at pH = 4 was narrow, with 91% of the particles having an equivalent diameter of 122 nm (Fig. 5B). Increasing the pH from 4 to 7.5 increased the particle sizes by a factor of 5.5, or from 120 ± 20 to 750 ± 50 nm (Fig. 5A). The particle size distribution also became broader with pH. At pH = 7, for example, 12.4% of the particles were 615 nm and increased in size to 955 nm (17.9%) (Fig. 5B).

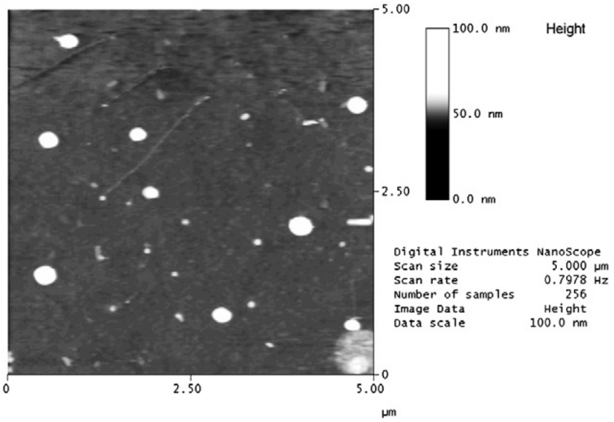

Fig. 3 – AFM image of the particles (in white) (0.003 M Fe^{2+}, pH = 6.3 and 1 kΩ external resistance).

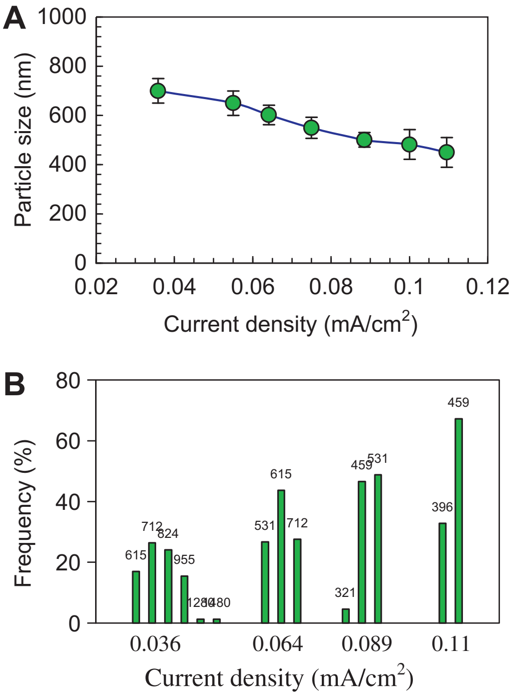

Fig. 4 – Effect of current on (A) particle size, and (B) particle size distribution at selected current densities (numbers indicate particle sizes in nm) (0.05 M NaCl, 0.06 M $NaHCO_3$, 0.007 M Fe^{2+}, and pH = 6.3).

The Fe^{2+} concentration also significantly affected particle sizes (Fig. 6A). When the Fe^{2+} concentration increased from 50 to 1000 mg/L, the particle size linearly increased from 402 ± 50 to 932 ± 50 nm. The size distribution at the lower Fe^{2+} concentrations tended to be less dispersed, with 90% particles 396 nm in equivalent diameter at 50 mg/L. At the very highest Fe^{2+} concentration of 1000 mg/L, the particle size distribution was broader, with 14.3% of the particles 712 nm and 6.3% of the particles 1280 nm (Fig. 6B).

These results show that it is possible to produce nano-sized particles of ferrihydrite (transforming to goethite) from AMD while at the same time producing electrical current. The ferric oxide particles were highly spherical, had paramagnetic properties, and particle size could be controlled by varying the operational parameters. Using a low pH or low concentration of Fe^{2+} (both resulting in low currents due to the lower rate of reaction) produced the smallest particles (120 nm). Under such conditions the maximum voltage was 0.06 V. With pH = 6.3 and 7 mM Fe^{2+}, a maximum power of 290 mW/m^2 was produced (0.64 A/m^2) (Cheng et al., 2007). These conditions produce ferric oxide particles rapidly with a size of 402 nm. Iron concentrations for AMD waters could be diluted using reactor effluent, and pH could be adjusted using various alkaline reagents, although the effect of chemical addition on the particles formed would need to be evaluated for specific AMD streams.

Practical applications of the technology for AMD treatment will require further development of systems that efficiently

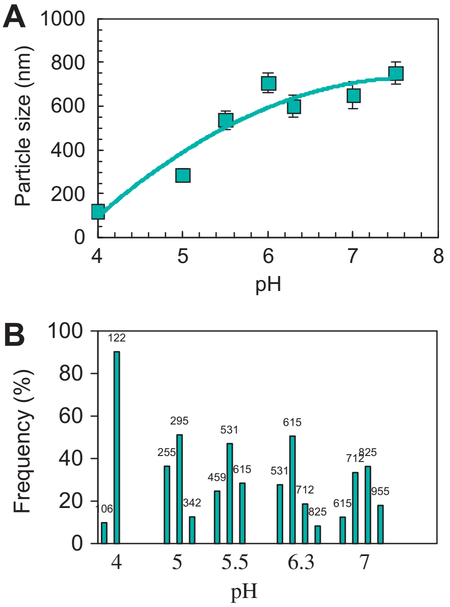

Fig. 5 – Effect of pH on (A) particle size and (B) and particle size distribution at selected pH conditions (numbers indicate particle sizes in nm) (0.05 M NaCl, 0.06 M $NaHCO_3$, 0.007 M Fe^{2+}, and 1 kΩ external resistance).

remove particles (for example through continuous centrifugation, that do not use precious metal electrodes, and that have electrodes with scalable architectures). Substantial progress is being made in these latter two topics based on the development of MFCs for wastewater treatment (Logan, 2010a, 2010b). For example, although the cathode contained a Pt catalyst, non-precious metals catalysts such as CoTMPP can be used as a catalyst (Zhao et al., 2005; Cheng et al., 2006). Recently cathodes that have been developed using activated carbon and no metal catalysts have achieved nearly equal performance to cathodes used here (Zhang et al., 2009). Scalable architectures for MFCs have been developed based on using high surface area graphite brush anodes and tubular cathodes (Zuo et al., 2007; Logan et al., 2007), providing increased surface areas per volume of reactor and thus the need for much less treatment times (Logan, 2008). The use of these electrodes and materials in AMD-FC reactors should enable scalable and more efficient systems for iron recovery, power generation, and AMD treatment.

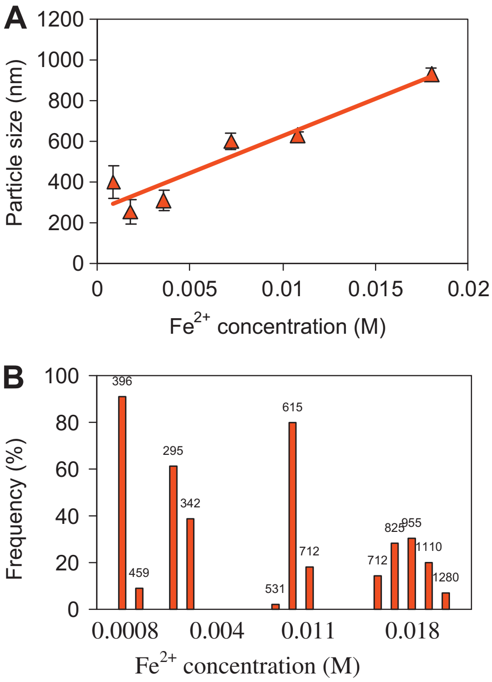

Fig. 6 – Effect of Fe^{2+} concentration on (A) particle size and (B) particle size distribution at selected Fe^{2+} concentrations (numbers indicate particle sizes in nm) (0.05 M NaCl, 0.06 M $NaHCO_3$, pH = 6.3, and 1 kΩ external resistance).

4. Conclusions

It is possible to use AMD types of soluble iron solutions in fuel cell-based technologies to create spherical nano-particles of iron oxide (ferrihydrite) that are transformed to goethite (α-FeOOH) upon drying. Particle diameters were controlled to be in the range of 120–700 nm by varying the conditions in the fuel cell, such as current density (0.04–0.12 mA/cm^2), pH (4–7.5), and initial Fe(II) concentration (50–1000 mg/L). These results provide a method to easily produce iron oxide particles that can be used in pigments and other products, although further research will be needed on many aspects of this process before these approaches could be successfully commercialized.

Acknowledgements

This research was supported by NSF Grant BES-0401885.

REFERENCES

Burleson, D.J., Penn, R.L., 2006. Two-step growth of goethite from ferrihydrite. Langmuir 22, 402–409.

Cheng, S., Dempsey, B.A., Logan, B.E., 2007. Electricity generation from synthetic acid-mine drainage (AMD) water using fuel cell technologies. Environmental Science & Technology 41 (23), 8149–8153.

Cheng, S., Liu, H., Logan, B.E., 2006. Power densities using different cathode catalysts (Pt and CoTMPP) and polymer binders (Nafion and PTFE) in single chamber microbial fuel cells. Environmental Science & Technology 40, 364–369.

Govaert, A., Dauwe, C., Plinke, P., De Grave, E., De Sitter, J., 1976. A classification of goethite minerals based on the Mőssbauer behaviour. Journal De Physique 37, C6-825-C6-827.

Jenke, D.R., Diebold, F.E., 1983. Recovery of valuable metals from acid-mine drainage by selective titration. Water Research 17, 1585–1590.

Jang, J.-H., Dempsey, B.A., Catchen, G.L., Burgos, W.D., 2003. Effects of Zn(II), Cu(II), Mn(II), NO_3^-, or SO_4^{-2} at pH 6.5 and 8.5 on transformation of hydrous ferric oxide (HFO) to more stable ferric oxides. Colloids Surfaces A 221, 55–68.

Kirby, C.S., Decker, S.M., Macander, N.K., 1999. Comparison of color, chemical and mineralogical compositions of mine drainage sediments to pigment. Environmental Geology 37, 243–254.

Kairies, C.L., Capo, C.L., Watzlaf, G.R., 2005. Chemical and physical properties of iron hydroxide precipitates associated with passively treated coal mine drainage in the Bituminous regions of Pennsylvania and Maryland. Applied Geochemistry 20, 1445–1460.

Kosmulski, M., Serge, D.V., Maczka, E., Rosenholm, J.B., 2004. Morphology of synthetic goethite particles. Journal of Colloid and Interface Science 271, 261–269.

Kim, H., Subramanian, N.P., Popov, B.N., 2004. Preparation of PEM fuel cell electrodes using pulse electrodeposition. Journal of Power Sources 138, 14–24.

Luengo, C., Brigante, M., Avena, M., 2007. Adsorption kinetics of phosphate and arsenate on goethite. A comparative study. Journal of Colloid and Interface Science 311, 354–360.

Lagarec, K. and Rancourt, D. G. (1998) Recoil: Mössbauer Spectral Analysis Software for Windows, version 1.01998.

Logan, B.E., 2010a. In: Rabaey, K., Angenent, L., Schröder, U., Keller, J. (Eds.), Bioelectrochemical Systems: From Extracellular Electron Transfer to Biotechnological Applications. IWA Publishing, London, pp. 184–204.

Logan, B.E., 2010b. Scaling up microbial fuel cells and other bioelectrochemical systems. Applied Microbiology and Biotechnology. doi:10.1007/s00253-00009-02378-00259.

Logan, B.E., Cheng, S., Watson, V., Estadt, G., 2007. Graphite fiber brush anodes for increased power production in air-cathode microbial fuel cells. Environmental Science & Technology 41 (9), 3341–3346.

Logan, B.E., 2008. Microbial Fuel Cells. John Wiley & Sons, Inc., Hoboken, NJ.

Matlock, M.M., Henke, K.R., Atwood, D.A., 2002. Effectiveness of commercial reagents for heavy metal removal from water with new insights for future chelate designs. Journal of Hazardous Materials 92, 129–142.

Penn, R.L., Erbs, J.J., Gulliver, D.M., 2006. Controlled growth of alpha-FeOOH nanorods by exploiting-oriented aggregation. Journal of Crystal Growth 293, 1–4.

Sepulveda-Guzman, S., Perez-Camacho, O., Rodrıguez-Fernandez, O., Garcıa-Zamora, M., 2005. In situ preparation of magnetic nanocomposites of goethite in a styrene–maleimide copolymer template. J Magnetism Magnetic Materials 294, e47–e50.

Tabak, H.H., Scharp, R., Burckle, J., Kawahara, F.K., Govind, R., 2003. Advances in biotreatment of acid mine drainage and biorecovery of metals: 1. Metal precipitation for recovery and recycle. Biodegradation 14, 423–436.

Wei, X.C., Viadero, R.C., 2007. Synthesis of magnetite nanoparticles with ferric iron recovered from acid mine drainage: implications for environmental engineering. Colloids Surfaces A 294, 280–286.

Wei, X.C., Viadero, R.C., Buzby, K.M., 2005. Recovery of iron and aluminum from acid mine drainage by selective precipitation. Environmental Engineering Science 22, 745–755.

Zhao, H., Stanforth, R.S., 2001. Competitive adsorption of phosphate and arsenate on goethite. Environmental Science & Technology 35, 4753–4757.

Zhao, F., Harnisch, F., Schröder, U., Scholz, F., Bogdanoff, P., Herrmann, I., 2005. Application of pyrolysed iron (II) phthalocyanine and CoTMPP based oxygen reduction catalysts as cathode materials in microbial fuel cells. Electrochemistry Communications 7, 1405–1410.

Zhang, F., Cheng, S., Pant, D., Bogaert, G.V., Logan, B.E., 2009. Power generation using an activated carbon and metal mesh cathode in a microbial fuel cell. Electrochemistry Communications 11 (11), 2177–2179.

Zuo, Y., Cheng, S., Call, D., Logan, B.E., 2007. Tubular membrane cathodes for scalable power generation in microbial fuel cells. Environmental Science & Technology 41 (9), 3347–3353.